Electronic Supplementary Material (ESI) for ChemComm.

Water-in-Salt Electrolytes – Molecular Insights to the High Solubility of Lithium-Ion Salts

Aleksandar Tot, Lars Kloo

Division of Applied Physical Chemistry, Department of Chemistry, KTH Royal Institute of Technology, Stockholm, SE-10044, Sweden

Electronic Supplementary Information

Solubility determination. The determination of Li[TFSI] solubility was performed by the shake-flask method. In the experiments, a double-layer glass vessel with a volume of 20 cm^3 was used. Small magnetic stirrers were added to each flask with a stirring speed of 100 rpm. The solubility measurements of Li[TFSI] saturated solutions were performed at temperatures between 288 to 323. The temperature was controlled by a Lauda thermostat with the standard uncertainty in determining the temperature of 0.01K. For each measurement, the solutions were stirred for 2 days and then rest without stirring for 24 h at the same temperature. The 0.5 cm^3 of the solution was taken by syringe filter (33 mm diameter sterile Millex-HA syringe filter with 0.45 mm pore size mixed cellulose esters membrane) fitted with a long needle. Samples were transferred to 5 cm^3 pre-weighed glass flasks and their mass was measured with an accuracy of $1 \cdot 10^{-5}$ g in the lower range. The samples were placed in a vacuum oven at 343.15 K and dried to recover the solid compound. The mass of the solute was determined gravimetrically, under the inert atmosphere in the glovebox. Each obtained value represents the average of at least five independent measurements. The relative standard uncertainty in the mass fraction solubility is 0.015%. Reproducibility was found to be better than 0.002.

XRD measurements. The X-ray diffraction measurements were carried out using a PANalytical X'Pert PRO diffractometer in Bragg-Brentano geometry with CuKα radiation at a wavelength λ = 1.54 Å. After the solubility measurements, the solid phase was collected, keep in the vacuum, and dried to remove residual water.

Raman measurements. The BioRad FTS 6000 with Raman accessory was used for measuring Raman spectra. The detector was Ge cooled with liquid nitrogen. The effective frequency range was 100-3600 cm^{-1}. Raman scattering was detected with CCD camera and spectral resolution was 4 cm^{-1}.

For calculation of excess Raman spectra, pure water and various samples with gradual increased concentration of Li[TFSI] (Table S3) were used. The spectral range was 2800 to 3600 cm^{-1}. The obtained spectra with increased concentration of Li-salt were subtracted from water and the positive peak was deconvoluted. From deconvoluted spectra the hydration spectra were calculated as an integral of obtained peak area (parameters are given in Table S4). The hydration number was calculated from obtained hydration spectra, using equation:

$$N_{\text{hydration}} = \frac{\int I_{\text{hydration}}(\nu)d\nu}{\int I_{\text{hydration}}(\nu)d\nu + \frac{\sigma_{\text{hydration}}}{\sigma_{\text{water}}} + \int I_{water}(\nu)d\nu} / \frac{n_{\text{Li[TFSI]}}}{n_{\text{water}}},$$

where $I_{\text{hydration}}$ represents the hydration spectra, obtained after deconvolution of excess spectra, I_{water} is integral of bulk water, $\sigma_{\text{hydration}}/\sigma_{\text{water}}$ is Raman cross section calculated from measured spectra (the obtained value was 0.75), while n_i represents the number of moles of corresponding species

Molecular dynamics simulations. Molecular dynamics (MD) simulations were conducted on the aqueous Li[TFSI] solutions with the various ratio between Li[TFSI] and water. The models were chosen to represent systems with the prominent solubility of Li[TFSI] (2 systems), with the number of molecules close to limiting solubility, and the 2 systems where the Li[TFSI] is not soluble. MD

simulations were performed using Tinker software and applying modified OPLS-AA force field. The force field used was validated by comparison to experimentally determined densities (Table S2). All simulated systems were created by replicating the Li[TFSI]-H_2O complexes using the xyzedit option in Tinker, which results in large simulation cells 70-100 Å. The simulation box dimensions were gradually decreased to 40-45 Å depending on the electrolyte composition during NPT equilibration runs at 333.15 K for 5-10 ns with longer runs used for increased content of water. Afterward, the simulation temperature was reduced to 298.15 K and electrolytes were equilibrated. The optimized electrolytes were further investigated by applying an NVT ensemble, using equilibrium box dimensions. The Ewald summation method was used for the electrostatic interactions. Multiple timestep integration was employed with an inner timestep of 0.5 fs (bonded interactions); a central time step of 1.5 fs for all nonbonded interactions within a truncation distance of 7.0-8.0 Å and an outer time step of 3.0 fs for all nonbonded interactions between 7.0 Å and the nonbonded truncation distance of the smaller of half of the simulation cell. Each simulation run was at least 50 ns. The temperature and the pressure were controlled by A Nose-Hoover thermostat and a barostat. The equilibrium time was excluded from the analysis of data, and the results of simulations were interpreted using the radial distribution functions (RDFs) and coordination numbers (CN). The radial distribution functions were calculated using the Tinker software, with the option radial, while the coordination numbers were calculated using the equation:

$$CN = 4\pi\rho\int_0^{r'} g(r)r^2 \mathrm{d}r$$

where ρ is the average density, $g(r)$ is the RDF, r' is the distance from the central atom. To study the dynamic coordination structure, the series of coordination numbers were evaluated for each time step by counting the number of oxygen atoms from water or $TFSI^-$ within cutoff distance of 3.5 Å from selected Li^+ ion or 4.0 Å from water oxygen.

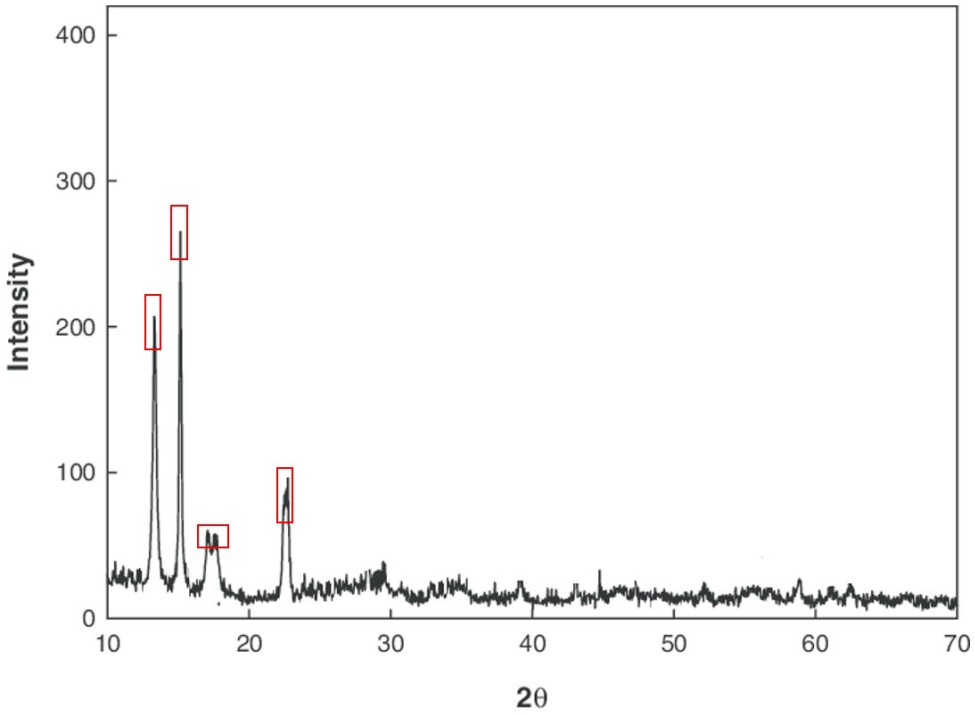

Figure S1. XRD pattern of white solid precipitate after the solubility measurements. The red squares represent the assigned peaks for Li[TFSI] powder.

Table S1. The molality and number of molecules used for each MD simulation run

Abbreviation	Molality (mol of Li[TFSI] / kg of water)	Number of Li[TFSI] molecules	Number of water molecules
$Li[TFSI]_{(1)}:H_2O_{(1)}$	55.55	190	190
$Li[TFSI]_{(1)}:H_2O_{(2)}$	27.78	190	380
$Li[TFSI]_{(1)}:H_2O_{(3)}$	18.51	190	570
$Li[TFSI]_{(1)}:H_2O_{(4)}$	13.89	190	760
$Li[TFSI]_{(1)}:H_2O_{(6)}$	9.26	190	950

Table S2. The molality and number of molecules used in each MD simulation run

Li[TFSI]:H_2O mole ratio $_{(sim)}$	$d_{(sim)}$ / g·cm^{-3}	Li[TFSI]:H_2O mole ratio $_{(exp)}$	$d_{(exp)}$ / g·cm^{-3}
1:3	1.694	1:2.98[a]	1.690
1:4	1.660	1:3.93[b]	1.654
		1:4.27[a]	1.636
1:6	1.554	1:7.40[a]	1.497

[a]Horwitz et al., *J. Chem. Thermodyn.*, 158 (2021) 106457

[b]Gilber et al., *J. Chem. Eng. Data*, 2017, **62**, 2056

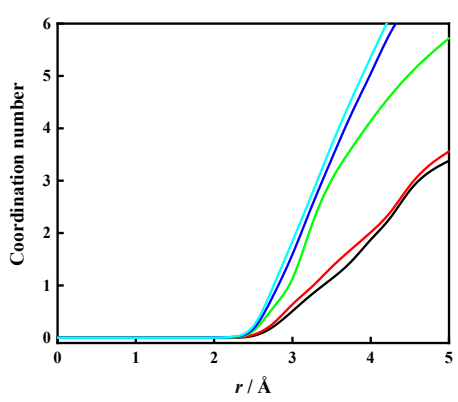

a)

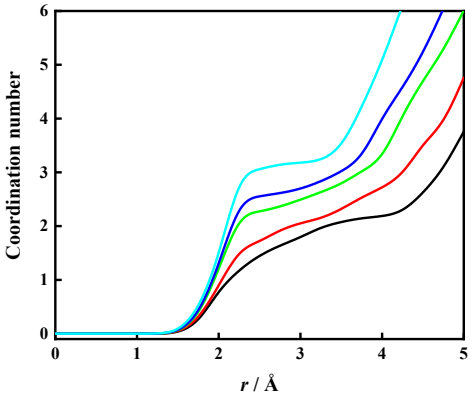

b)

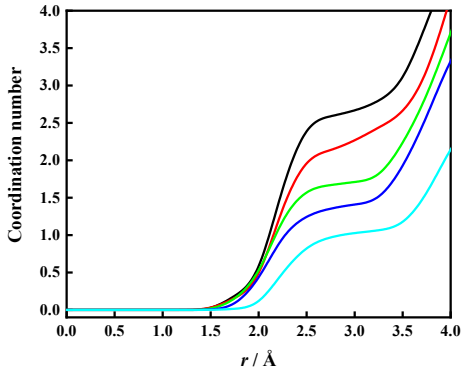

c)

Figure S2. The coordination number of water O-O atoms (a), O(water)-Li^+ (b) and O(TFSI)-Li^+ (c). Black - $Li[TFSI]_{(1)}:H_2O_{(1)}$; red – $Li[TFSI]_{(1)}:H_2O_{(2)}$; green - $Li[TFSI]_{(1)}:H_2O_{(3)}$; blue – $Li[TFSI]_{(1)}:H_2O_{(4)}$; cyano – $Li[TFSI]_{(1)}:H_2O_{(6)}$

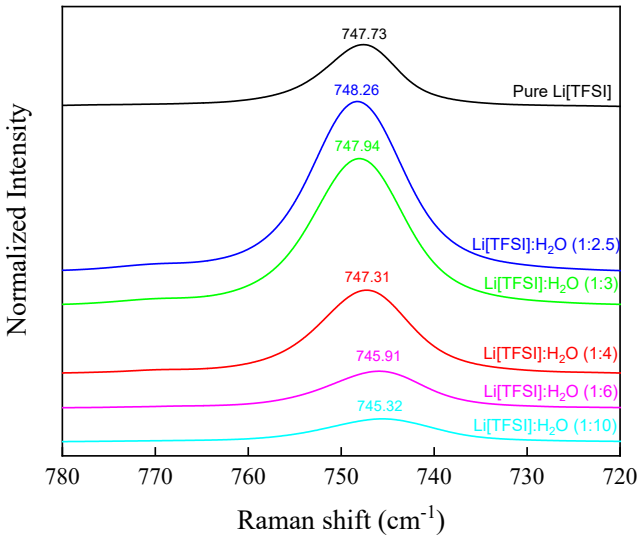

Figure S3. The change of the Raman S-N-S bending vibration with concentration

Table S3. The systems used for Raman measurements

Abbreviation	Molality (mol of Li[TFSI] / kg of water)	Li[TFSI]:H_2O mole ratio
$Li[TFSI]_{(1)}:H_2O_{(2.5)}$	22.22	1:2.5
$Li[TFSI]_{(1)}:H_2O_{(3)}$	18.52	1:3
$Li[TFSI]_{(1)}:H_2O_{(4)}$	13.89	1:4
$Li[TFSI]_{(1)}:H_2O_{(6)}$	9.26	1:6
$Li[TFSI]_{(1)}:H_2O_{(10)}$	5.56	1:10
$Li[TFSI]_{(1)}:H_2O_{(15)}$	3.71	1:15
$Li[TFSI]_{(1)}:H_2O_{(20)}$	2.78	1:20

Table S4. The parameters of integration

Abbreviation	Area	Peak width at the half height
Water	44735.5	218.02
$Li[TFSI]_{(1)}:H_2O_{(2.5)}$	4087.82	109.73
$Li[TFSI]_{(1)}:H_2O_{(3)}$	6664.19	106.47
$Li[TFSI]_{(1)}:H_2O_{(4)}$	13357.7	94.143
$Li[TFSI]_{(1)}:H_2O_{(6)}$	18720.4	86.362
$Li[TFSI]_{(1)}:H_2O_{(10)}$	19760.7	87.816
$Li[TFSI]_{(1)}:H_2O_{(15)}$	20816.7	89.649
$Li[TFSI]_{(1)}:H_2O_{(20)}$	23128.5	102.50

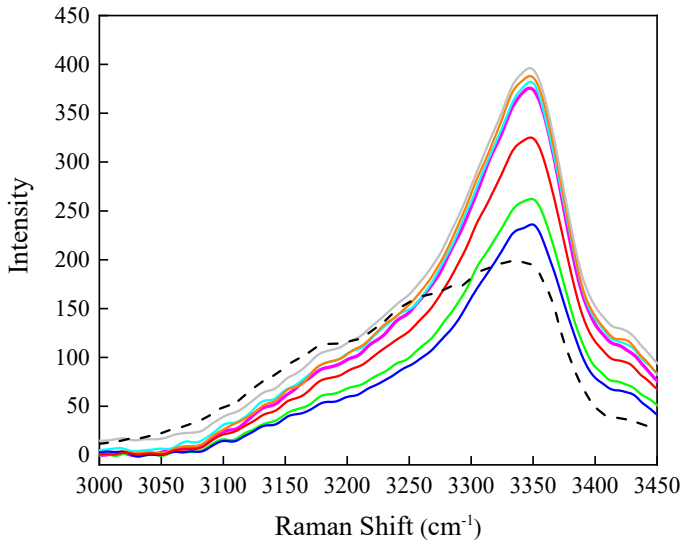

Figure S4. The Raman spectra of O-H stretching vibration. Black - water; blue – $Li[TFSI]_{(1)}:H_2O_{(2.5)}$; green - $Li[TFSI]_{(1)}:H_2O_{(3)}$; red – $Li[TFSI]_{(1)}:H_2O_{(4)}$; magenta – $Li[TFSI]_{(1)}:H_2O_{(6)}$; cyan - $Li[TFSI]_{(1)}:H_2O_{(10)}$; orange - $Li[TFSI]_{(15)}:H_2O_{(1)}$; gray - $Li[TFSI]_{(1)}:H_2O_{(20)}$

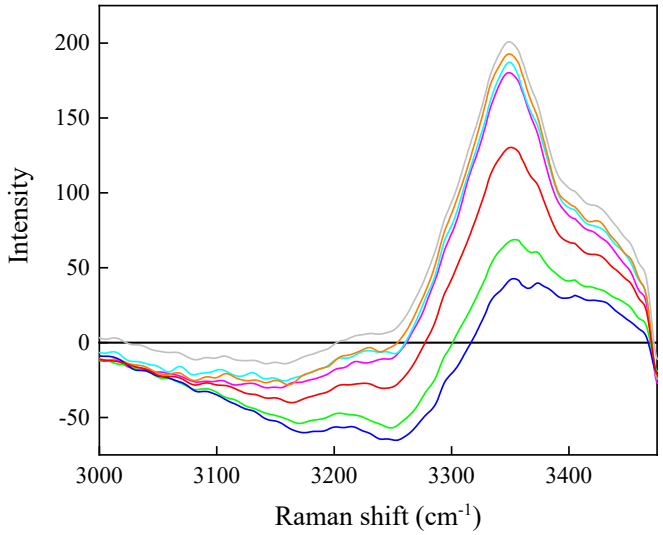

Figure S5. The excess Raman spectra of O-H stretching vibration. Blue – $Li[TFSI]_{(1)}:H_2O_{(2.5)}$; green - $Li[TFSI]_{(1)}:H_2O_{(3)}$; red – $Li[TFSI]_{(1)}:H_2O_{(4)}$; magenta – $Li[TFSI]_{(1)}:H_2O_{(6)}$; cyan - $Li[TFSI]_{(1)}:H_2O_{(10)}$; orange - $Li[TFSI]_{(15)}:H_2O_{(1)}$; gray - $Li[TFSI]_{(1)}:H_2O_{(20)}$

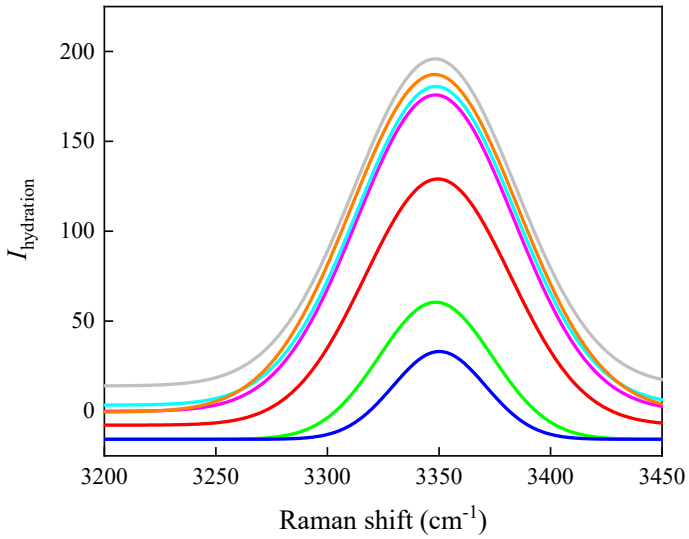

Figure S6. The deconvoluted $I_{hydration}$ Raman spectra. Blue – $Li[TFSI]_{(1)}:H_2O_{(2.5)}$; green - $Li[TFSI]_{(1)}:H_2O_{(3)}$; red – $Li[TFSI]_{(1)}:H_2O_{(4)}$; magenta – $Li[TFSI]_{(1)}:H_2O_{(6)}$; cyan - $Li[TFSI]_{(1)}:H_2O_{(10)}$; orange - $Li[TFSI]_{(15)}:H_2O_{(1)}$; gray - $Li[TFSI]_{(1)}:H_2O_{(20)}$